


Effects of Loops and Nucleotides in G-Quadruplexes on Their Interaction with an Azacalixarene, Methylazacalix[6]pyridine

Ai-Jiao Guan,^{†,§} En-Xuan Zhang,[‡] Jun-Feng Xiang,[†] Qian Li,^{†,§} Qian-Fan Yang,[†] Lin Li,^{†,§} Ya-Lin Tang,^{*,†} and Mei-Xiang Wang^{*,‡}

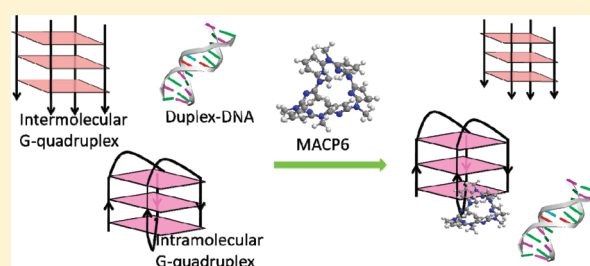
[†]Beijing National Laboratory for Molecular Sciences, Center for Molecular Sciences, State Key Laboratory for Structural Chemistry of Unstable and Stable Species, Institute of Chemistry, Chinese Academy of Sciences, Beijing, 100190, P. R. China

[‡]Department of Chemistry, Tsinghua University, Beijing 100084, P. R. China

[§]Graduate University of the Chinese Academy of Sciences, Beijing 100049, P. R. China

 Supporting Information

ABSTRACT: A novel trend in G-quadruplex ligand design is to build a binder that is able to not only discriminate G-quadruplex from duplex-DNA, but also among various G-quadruplex structures. Methylazacalix[6]pyridine (MACP6), a new type of azacalixarene with flexible conformation, exhibits induced circular dichroism signals when interacted with most of G-quadruplexes. The intensities of the induced signals are strongly dependent on the topology of G-quadruplexes. Further evidence has shown that these signals can be ascribed to the preferred binding of MACP6 to the loops of G-quadruplexes, which rely on the nature of nucleotides in the loops.



INTRODUCTION

Guanine-rich DNA sequences, which are particularly found in the regions of telomere and gene promoters, can fold into G-quadruplex structure. The formation of G-quadruplex at the telomeric end can prevent telomere elongation by telomerase,¹ which is activated in 80–85% cancer cells, thus leading to inhibition of telomerase activity.^{2,3} In addition, G-quadruplex-forming sequences have been identified in the promoter regions of human oncogene related to the regulation of gene transcriptional level and biological dysfunctions that selectively alter the integrity of cancer cells.^{4–6} Therefore, a ligand inducing the G-quadruplex formation and/or stabilizing G-quadruplex structure may be a potential anticancer agent.⁷

Recently, the field of G-quadruplex ligands has developed dramatically and a number of ligands have been reported. Most ligands capable of interaction with the G-tetrad via π – π stacking and electrostatic interaction contain a polyaromatic heterocyclic ring system with protonable side arms or positive charge.^{7–9} For example, PIPER and RHPS4 bind to the quadruplex by stacking on the terminal G-quartet.^{10,11} Pentacationic manganese(III) porphyrin shows very high affinity for the G-quadruplex structure due to stacking interaction with the terminal tetrad and electrostatic interaction between the central Mn^{3+} ion and the carbonyl oxygen.¹² On the other hand, other ligands without the above features have also been found to be able to stabilize G-quadruplex. For example, nonaromatic alkaloids increase the melting temperature of G-quadruplex by more than 10 °C,^{13,14} while a scissors-shaped molecule, NPA, does so by about 4–9 °C.¹⁵ Telomestatin, a neutral macrocyclic molecule, is one of the most

interesting ligands that show a high stability (24 °C) and selectivity (more than 70-fold) for G-quadruplex over duplex-DNA.^{16,17} Oxazole-based peptide macrocycles¹⁸ and HXDV¹⁹ are also found to bind to G-quadruplex with high selectivity. These results suggest the potential discovery of G-quadruplex ligands from macrocycle compounds with novel structure. Calixarenes are macrocyclic compounds with special size of cavity and flexible conformation, which makes them popular scaffolds for molecular recognition and drug design.^{20–23} Azacalixarene, a new class of calixarene, has aroused our interest in molecular recognition. Herein, we present such investigations on the interaction between G-quadruplexes and a new type of azacalixarene, methylazacalix[6]pyridine²⁴ (MACP6) (Figure 1). Surprisingly, MACP6 shows a notable discrimination between various G-quadruplexes and duplex DNA, which may be ascribed to its preferred binding to the loops in G-quadruplexes correlated with the bases' nature in the loops. These results provide helpful information about constructing novel macrocycle-based G-quadruplex ligands.

MATERIALS AND METHODS

Materials and Sample Preparation. MACP6 was synthesized according to the literature,²⁵ and the purity was proved by mass spectrometry and nuclear magnetic resonance (Figures S1–S2 in the Supporting Information). Calf thymus DNA (CT;

Received: May 5, 2011

Revised: September 14, 2011

Published: September 16, 2011

Cat. No. 15633-019) was purchased from Invitrogen Biotechnology Co. Ltd. and used without further purification. All oligonucleotides were purchased from Invitrogen Biotechnology Co. Ltd. (Beijing, China), and purified by polyacrylamide gel electrophoresis (PAGE) (purity 98%).

The stock solution of MACP6 was prepared by dissolving in dimethyl sulfoxide (DMSO). The stock solution of CT was diluted by 70 mM KCl, 20 mM phosphate buffer solution ($\text{K}_2\text{HPO}_4/\text{KH}_2\text{PO}_4$) at pH 7.05. The G-quadruplexes of c-kit,²⁶ c-myc 2345,²⁷ TBA (thrombin binding DNA aptamer),²⁸ bcl-2 2345,⁶ H22,²⁹ A24,³⁰ H22-Form 1,³¹ H22-Form 2,^{32,33} U6,³⁴ U1B7,³⁴ T12,³⁵ and H7³⁶ (Table 1) were prepared following the literature. All samples were heated to 358 K for 15 min and then slowly cooled to room temperature. The concentration of each DNA sample was determined from absorbance extinction coefficient at 260 nm at 298 K before analysis. Other chemicals were of analytical reagent grade, and ultrapure water was used throughout the experiments. The measured samples identified by circular dichroism (CD) were prepared by mixing a quantity of MACP6 solution with DNA solution. The concentration of DMSO was 1% (v/v).

Spectral Measurement. Absorption spectra were collected with a 5-mm path-length cell on an Agilent 8453 UV–vis spectrophotometer. CD measurement was carried out on a Jasco-815 spectropolarimeter in a 1-cm path-length cell, with a scan speed of 1000 nm/min, a response time of 0.5 s, and a 2 nm bandwidth from 600 to 200 nm. Each spectrum was the average of three scans and corrected by buffer solution.

NMR Experiment. NMR experiments were performed on a Bruker AVANCE 600 spectrometer equipped with a 5 mm BBI probe capable of delivering z-field gradients. All experiments were carried out at 298.2 K. The ^1H NMR spectra were recorded

by the pulse program p3919gp that applied 3–9–19 pulses with gradients for water suppression, 512 scans were acquired for each spectrum with a relaxation delay of 2 s. For each sample, trimethylsilyl propionate (TSP) was added as a reference of chemical shift.

Molecular Modeling Studies. Qualitative molecular modeling was carried out using AutoDock (v4.0) software. The G-quadruplex structures of the c-kit, myc22-G14T/G23T, TBA, bcl-2 2345, T12 and H7 with available solution structures were obtained from the Protein Data Bank and the PDB IDs were 2O3M,²⁶ 1XAV,³⁷ 148D,⁴ 2F8U,⁶ 1K8P³⁸ and 1NP9,³⁶ respectively. Before the docking process, MACP6 and G-quadruplexes were optimized in a CHARMM force-field in Insight II 2005 (Accelrys, Inc.). A grid with a default volume of $22.5 \times 22.5 \times 22.5$ Å and with a spacing of 0.375 Å centered on the binding site of G-quadruplex was prepared. The maximum number of energy evaluations and GA run is set to 2 500 000 and 100, respectively.

RESULTS AND DISCUSSION

Interaction between MACP6 and G-Quadruplexes. MACP6 is an achiral molecule, and exhibits no intrinsic CD signal in either DMSO or phosphate buffer solution, which can be ascribed to its facile transformation among different conformations.^{24,39} C-kit G-quadruplex, formed from the DNA sequence in the promoter region of the c-kit oncogene,²⁶ shows no CD signal longer than 300 nm because of no absorption for DNA. However, addition of c-kit quadruplex into MACP6 phosphate buffer solution gives rise to the appearance of two intense signals at the wavelength longer than 300 nm (Figure 2a): a positive band at 385 nm and negative one at 345 nm, corresponding to positive Cotton effect.⁴⁰ Clearly, these new CD signals should arise from MACP6 through the interaction with c-kit G-quadruplex since only MACP6 and MACP6–quadruplex solution exhibit absorption at wavelengths above 300 nm (Figure 2b).

Generally, G-quadruplexes interact with their ligands through face stacking, loop, edge or groove binding.⁴¹ The weak intensity of the induced CD is typical for DNA face stacking,¹⁰ while a large positive induced CD spectral changes together with small absorbance changes for minor-groove binding.⁴² Clearly, these features could not account for the intense induced positive Cotton effect and minor absorbance changes of MACP6 upon addition of quadruplex (Figure 2). In fact, the resonances of all imino protons of c-kit G-quadruplex were not affected in the

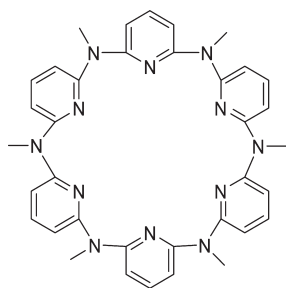


Figure 1. Structure of MACP6.

Table 1. The Abbreviation of Sequences and Topologies of G-Quadruplexes^a

| abbr. | sequences | motifs |
|------------|-------------------------------------|--------------------------------------|
| c-kit | [5'-AGGGAGGGCGCTGGGAGGAGGG-3'] | intramolecular parallel |
| c-myc 2345 | [5'-TGAGGGTGGGGAGGGTGGGGAA-3'] | |
| bcl-2 2345 | [5'-GGGCGCGGGAGGAATTGGGCGGG-3'] | intramolecular hybrid |
| H22-Form2 | [5'-AGGGTTAGGGTTAGGGTTAGGG-3'] | |
| H22-Form1 | [5'-TAGGGTTAGGGTTAGGGTTAGGG-3'] | |
| TBA | [5'-GGTTGGTGTGGTTGG-3'] | intramolecular antiparallel |
| A24 | [5'-TTAGGGTTAGGGTTAGGGTTAGGG-3'] | |
| H7 | [5'-TTAGGGT-3'] | intermolecular parallel |
| U6 | [5'-TAGGGUTAGGGT-3'] | |
| U1B7 | [5'-UAGGGT ^{Br} UAGGGT-3'] | intermolecular antiparallel |
| T12 | [5'-TAGGGTTAGGGT-3'] | intermolecular parallel/antiparallel |
| CT | calf thymus DNA | double strand |

^a G-quadruplex of A24 was formed in pbs- Na^+ solution, and the other G-quadruplexes were formed in pbs- K^+ solution.

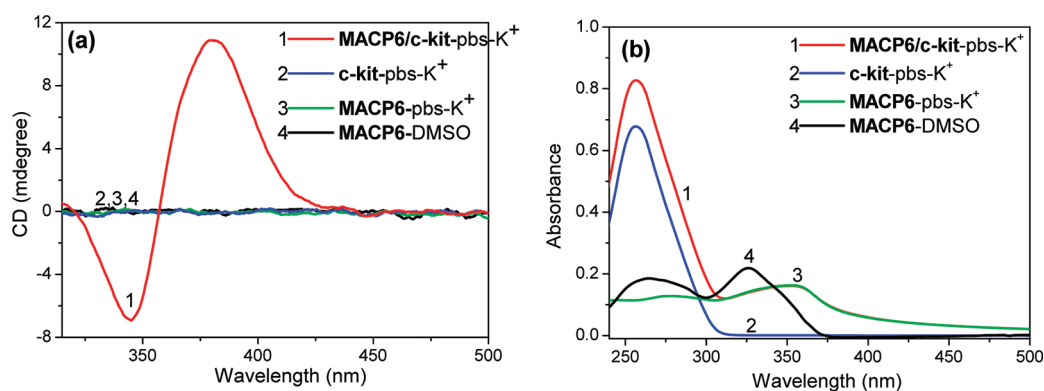


Figure 2. The CD (a) and absorption (b) spectra of 4 μM MACP6 and 4 μM c-kit G-quadruplex in pbs-K⁺ (curve 1), 4 μM c-kit G-quadruplex in pbs-K⁺ (curve 2), 4 μM MACP6 in pbs-K⁺ (curve 3) and 4 μM MACP6 in DMSO (curve 4).

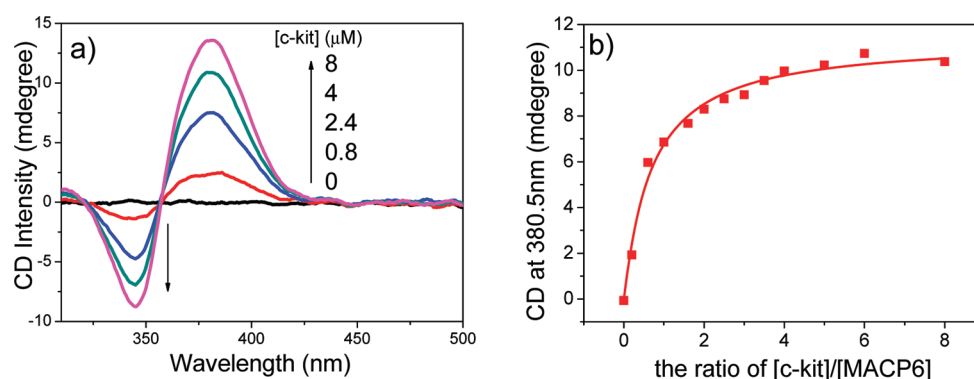


Figure 3. (a) The CD spectra of 4 μM MACP6 with different concentrations of c-kit G-quadruplex in 90 mM pbs-K⁺; (b) The fitting plot of the CD spectral changes of MACP6 at 380.5 nm against the ratio of [c-kit]/[MACP6].

presence of MACP6 (Figure S3 in the Supporting Information), indicating that face stacking or groove binding may not occur in the MACP6-quadruplex system.^{10,26} On the other hand, groove binding can be excluded because the size of MACP6 ($18 \times 12 \times 7.4 \text{ \AA}$)²⁰ is much larger than that of a G-quadruplex groove.^{38,43} This speculation was further proved by the fact that there was no induced CD signal of MACP6 in the presence of duplex CT (Figure S4 in the Supporting Information). Evidently, the structural features-nonplanar frame and steric hindrance of MACP6 cannot enable it to bind to G-quadruplex through face-stacking or groove binding.

Furthermore, the intensities of the induced CD signals of MACP6 increased with increasing the concentration of c-kit G-quadruplex (Figure 3a). With titration of more c-kit G-quadruplex, saturation of the induced CD signal of MACP6 was observed, and a plot of the CD intensity at 380.5 nm versus the ratio of [c-kit]/[MACP6] is shown in Figure 3b. Similar behaviors have been observed for all G-quadruplexes studied (Figures S5–S14 in the Supporting Information) and the plots are given in Figure S15 in the Supporting Information.

Additionally, quantitative evaluation of the interactions between MACP6 and the various forms of G-quadruplexes were carried out⁴⁴ by supposing the association constant, K as

$$K = \frac{[\text{GM}]}{[\text{G}] \cdot [\text{M}]} \quad (1)$$

with [GM], [G], and [M] representing the concentration of the complex, the free G-quadruplex and MACP6, respectively. If $[\text{G}]_0$ and $[\text{M}]_0$ denote the total concentration of G-quadruplex and MACP6.

$$[\text{G}] = [\text{G}]_0 - [\text{GM}] \quad (2)$$

$$[\text{G}] = [\text{G}]_0 - [\text{GM}] \quad (3)$$

and

$$[\text{GM}] = K \times ([\text{G}]_0 \times [\text{M}]_0 - [\text{G}]_0 \times [\text{GM}] - [\text{M}]_0 \times [\text{GM}] + [\text{GM}]^2) \quad (4)$$

then

$$[\text{GM}]^2 - ([\text{G}]_0 + [\text{M}]_0) \times [\text{GM}] + [\text{G}]_0 \times [\text{M}]_0 = \frac{[\text{GM}]}{K} \quad (5)$$

Since MACP6 and G-quadruplex alone have no CD signal longer than 300 nm, the intensity of the observed CD signal (experimental ellipticity, Ψ) could be related to the concentration of the complex as

$$\Psi = [\text{GM}] \times r \times l \quad (6)$$

Table 2. The r and K of [GM] Complexes Calculated According to eqs 5 and 7

| abbr. | $r/10^3$ [degree·cm ⁻¹ ·M ⁻¹] | $K/10^6$ [M ⁻¹] |
|------------|--|-----------------------------|
| c-kit | 2.62 ± 0.09 | 3.94 ± 0.30 |
| c-myc 2345 | 2.56 ± 0.11 | 2.46 ± 0.51 |
| bcl-2 2345 | 0.24 ± 0.02 | 0.41 ± 0.02 |
| H22-Form2 | 0.17 ± 0.005 | 1.43 ± 0 |
| TBA | 0.49 ± 0.07 | 0.09 ± 0.01 |
| A24 | 0.30 ± 0.02 | 0.38 ± 0 |
| H7 | 0.13 ± 0.002 | 0.30 ± 0.01 |
| U6 | 0.39 ± 0.01 | 0.98 ± 0.12 |
| U1B7 | 0.07 ± 0.01 | 1.18 ± 0 |
| T12 | 0.14 ± 0.02 | 1.21 ± 0.004 |

where r is the induced molar ellipticity coefficient of the complex in a 1-cm cell, and l is the path-length in centimeters. Then

$$[\text{GM}] = \frac{\Psi}{r \times l} \quad (7)$$

By combining eqs 5 and 7, one can obtain the values of r and K (see Table 2 and the Supporting Information) by adding the observed experimental ellipticity and the corresponding concentration of MACP6 and G-quadruplexes.

Judging from Table 2, one can see that MACP6 complexed with c-kit and c-myc G-quadruplexes showed larger binding constants (K) and induced molar ellipticity coefficient (r) than those interacted with other G-quadruplexes, suggesting that MACP6 can discriminate intramolecular parallel G-quadruplexes from others motifs. Clearly, the topologies of G-quadruplexes play an important role in their binding to MACP6.

Loop and Nucleotide Effect. G-quadruplex structures can be classified as intermolecular or intramolecular parallel, antiparallel, or hybrid conformations according to their strand polarities and the location of the loops that link the guanine strand(s) for quadruplexes formed either from a single-strand or from two strands.^{40,45,46} Since the major difference of the quadruplex topologies is concerned largely with loop structure, the effect of loop structure on the induced CD signals of MACP6 has been evaluated by the mutation of base group in two typical DNA sequences: c-myc 2345 and c-kit. Our choice is based on the relatively deep understanding of these DNA quadruplex structures^{5,26,27,37,47–49} as well as relatively large induced CD signals of MACP6 by these two G-quadruplexes.

C-myc 2345 forms an intramolecular propeller-type parallel-stranded G-quadruplex in K⁺-containing solution.²⁷ By mutation of several nucleotides, the loop topologies of c-myc 2345 can be modified while the central G-quadruplex structure remains unchanged (Table 3). For example, compared with that of c-myc 2345, the G-quadruplex of c-mycTGA-de possess the same central double-chain reversal loop while no edge side loop (T1G2A3) at the 5'-end due to the removal of TGA nucleotides from the main sequence. C-myc 1245 G-quadruplex has a longer central loop (T11T12T13T14T15A16) compared to that of c-myc 2345 (G11A12) (Figure 4b). However, under the same conditions, the CD spectra of MACP6 showed a dramatically different behavior in the presence of c-myc 2345, c-myc 1245, and c-mycTGA-de G-quadruplex: a slightly less intense CD signal of MACP6 with c-mycTGA-de G-quadruplex, while a

Table 3. DNA Sequence of the c-kit and c-myc Derivatives

| abbr. | sequences |
|----------------------------|--------------------------------------|
| c-myc 1245 ²⁷ | [5'-TGAGGGTGGG TTTTGA GGGTGGGGAA-3'] |
| c-myc 2345 ²⁷ | [5'-TGAGGGTGGG GA GGGTGGGGAA-3'] |
| c-myc TGA-de ³⁷ | [5'-GGGTGGG GA GGGTGGGGAA-3'] |
| c-kit ²⁶ | [5'-AGGG AGGG CGCT GGG AGG AGGG-3'] |
| c-kitA5T ²⁶ | [5'-AGGG TGGG CGCT GGG AGG AGGG-3'] |
| c-kitC9T ²⁶ | [5'-AGGG AGGG TGCT GGG AGG AGGG-3'] |
| c-kitG20T ²⁶ | [5'-AGGG AGGG CGCT GGG AGG ATGG-3'] |
| c-kitA5T/C9T ²⁶ | [5'-AGGG TGGG TGCT GGG AGG AGGG-3'] |

dramatically weaker CD signal with c-myc 1245 compared to those with c-myc 2345 (Figure 4a). These results indicated that the central double-chain reversal loop (G11A12) of c-myc also played a critical role in binding of MACP6.

Besides c-myc G-quadruplex, studies on the interaction of c-kit derivatives with MACP6 have also been investigated (Table 3). Although certain nucleotides in the loops were substituted, the parallel conformation of c-kit G-quadruplex remains: two single-residue double-chain reversal loops (A5, C9), one five-residues stem-loop (A16G17G18A19G20), and one two-residue loop (C11T12).²⁶ Obviously, c-kitA5T/C9T G-quadruplex caused dramatic reduction of the CD signal of 4 μM MACP6 compared to that of c-kit (Figure 5), which should be ascribed to the substitution of the fifth adenine and ninth cytosine by thymine. Additionally, reduction of the CD signal intensity of 4 μM MACP6 was also observed in the presence of c-kitC9T and c-kitA5T G-quadruplexes, where the fifth adenine and ninth cytosine were substituted by thymine respectively. These results evidenced that interaction of MACP6 with c-kit-derivative quadruplexes depended on the base nature at loops A5 and C9. On the other hand, substitution of G20T (c-kitG20T) at the stem loop (A16G17G18A19G20) resulted in a minor change of the induced CD signal of MACP6, which indicated a small contribution of the stem loop binding. Hence, MACP6 prefers to bind to the single-residue double-chain reversal loop (A5 and C9). Therefore, the preferred binding of MACP6 to intramolecular parallel G-quadruplex c-kit and c-myc mentioned in Table 2 should mainly be ascribed to the conformation of loops and type of nucleotide.

Molecular Modeling. For a clear understanding of the binding sites of various G-quadruplexes interacted with MACP6, qualitative molecular modeling using AutoDock (v.4.0) software were carried out, and the docking results showed good support with the above experimental data. In the docking of all possible active sites (G-quartet planes, side loops, and edges) of loops containing G-quadruplex of c-kit, c-myc22-G14T/G23T, TBA, and bcl-2 2345, the results showed that loop binding of MACP6 had the largest binding constant (Table 4 and Tables S1–S3 in the Supporting Information). Judging from the docking results of the c-kit/MACP6 system, MACP6 shows a preferential binding to the cavity of the single-residue double-chain reversal loops of A5 and C9 in c-kit G-quadruplex (Figure 6), which is consistent with the above CD results.

Discrimination of the Antiparallel/Hybrid Structures of H22 and Parallel/Antiparallel of T12. It has been reported that human telomeric sequence H22 d[AGGG(TTAGGG)₃] could adopt various intramolecular G-quadruplexes in different experimental conditions: antiparallel basket-type G-quadruplex in Na⁺ solution (Figure 7a),⁵⁰ parallel propeller form for K⁺ crystal,³⁸

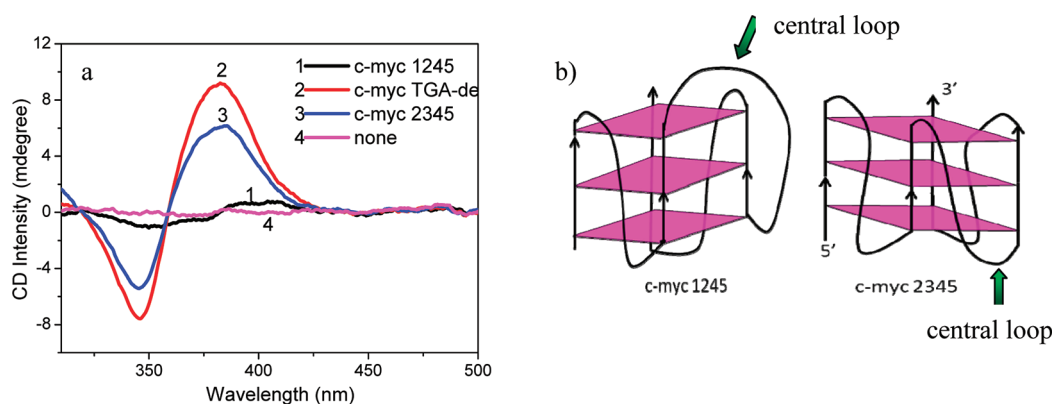


Figure 4. (a) The CD spectra of 4 μM MACP6 with 4 μM c-myc G-quadruplex derivatives in 90 mM pbs- K^+ . (b) The NMR-based topologies of the DNAs of c-myc1245 and c-myc2345.

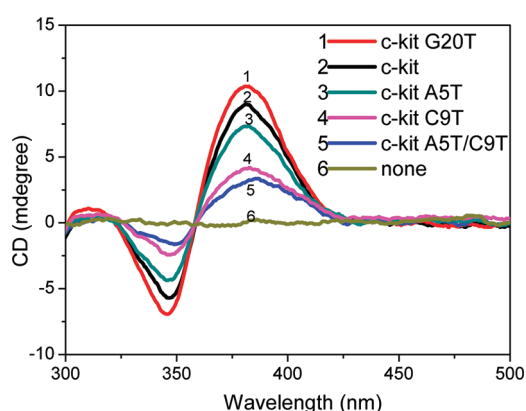


Figure 5. The CD spectra of 4 μM MACP6 with 4 μM c-kit G-quadruplex derivatives in 90 mM pbs- K^+ .

Table 4. Docking Results of MACP6 and c-kit PDB (ID 2O3M)

| S.NO | centroid of binding site | p KI | $\Delta G_{\text{binding}}$ kJ/mol |
|------|--------------------------|------|------------------------------------|
| 1 | A5 | 4.94 | −28.20 |
| 2 | A5-C9 | 4.91 | −28.03 |
| 3 | G2-G6-G10-G13 | 4.88 | −27.86 |
| 4 | A1-C11-T12 | 4.71 | −26.89 |
| 5 | A16-G17-G18-A19-G20 | 4.52 | −25.80 |
| 6 | G4-G8-G22-G15 | 4.36 | −24.89 |
| 7 | C9 | 4.31 | −24.61 |
| 8 | C11-T12 | 4.04 | −23.06 |

and (3 + 1) hybrid topology Form 1 (Figure 7b)³¹ and Form 2 (Figure 7c)^{32,33} in K^+ solution. Herein, we investigated whether MACP6 could discriminate the antiparallel/hybrid structure of H22 in solution. To get a single configuration, natural human telomeric sequences d[TAGGG(TTAGGG)₃] and d[TAGGG(TTAGGG)₃TT], which form predominantly hybrid Form 1 and Form 2 in K^+ solution, respectively, were used. As shown in Figure 8, the induced CD signals at 300–400 nm of MACP6 varies greatly when mixed with G-quadruplexes of antiparallel H22, hybrid Form 1, or hybrid Form 2, respectively. Under the same K^+ -containing solution, almost no induced CD signal of MACP6 was observed in the presence of hybrid Form 1, while negative Cotton effect⁴⁰ of MACP6—a positive band at 345 nm

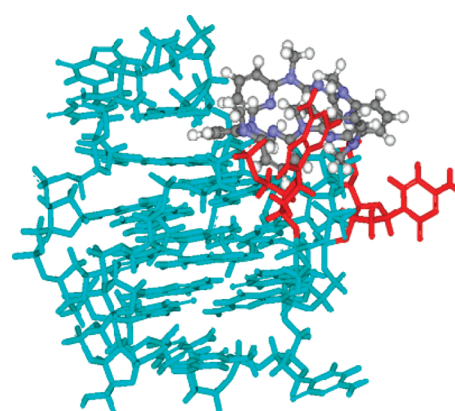


Figure 6. The plots of docked structure of MACP6–c-kit complex. The loops involved in the interaction are marked red. MACP6 is colored gray in the ball and stick mode.

and a negative one at 377 nm—was induced by hybrid Form 2 (Figure 8 and Figures S13–S14 in the Supporting Information). On the other hand, positive Cotton effect⁴⁰ of MACP6—a negative band at 345 nm and a positive one at 380 nm—was induced by the basket-type antiparallel H22 G-quadruplex in Na^+ solution. These results indicated that qualitative discrimination of MACP6 among the hybrid (3 + 1) and antiparallel topologies of H22 in solution could be achieved. However, the inversed CD signal of MACP6 induced by H22 hybrid Form 2 makes it difficult to determine the native ratio of antiparallel/hybrid for H22.

The two-repeat human telomeric sequence T12 d(TAGGGT-TAGGGT) can form both intermolecular parallel and antiparallel G-quadruplexes in K^+ -containing solution.³⁴ To identify the binding characteristics of MACP6 with parallel and antiparallel T12 G-quadruplex, the modified sequence U6 d(TAGGGUTAGGGT) and U1B7 d(UAGGGT^{Br}UAGGGT) were used, which forms a predominant parallel dimeric³⁴ and antiparallel dimeric⁵¹ G-quadruplex in K^+ -containing solution, respectively. Both G-quadruplexes of U6 and U1B7 can induce the CD signal of MACP6 (Figure S16–S17 in the Supporting Information). Plot in Figure 9 indicated that only little CD difference exists between the parallel and antiparallel T12 G-quadruplexes on MACP6. Therefore, MACP6 cannot determine the ratio of parallel/antiparallel for T12.

In conclusion, the first observation of interaction between MACP6 with G-quadruplex was made, and its preferential

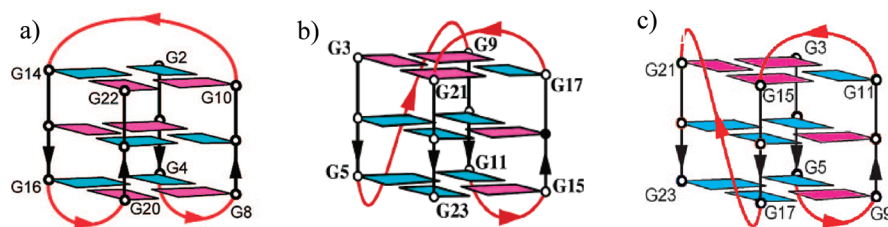


Figure 7. Schematic structures of intramolecular G-quadruplexes formed by four-repeat human telomeric sequences: (a) antiparallel basket-type form for d[AGGG(TTAGGG)₃] in Na⁺ solution,⁵⁰ (b) (3 + 1) Form 1 for d[TAGGG(TTAGGG)₃] in K⁺ solution,³¹ and (c) (3 + 1) Form 2 for d[TAGGG(TTAGGG)₃TT] in K⁺ solution.^{32,33}

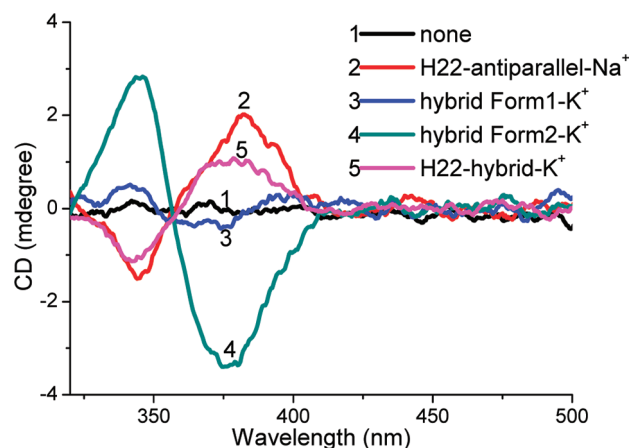


Figure 8. The CD spectra of 4 μ M MACP6 with 4 μ M G-quadruplex of antiparallel H22 in 100 mM pbs-Na⁺, hybrid Form 1 in 90 mM pbs-K⁺, and hybrid Form 2 in 90 mM pbs-K⁺, respectively.

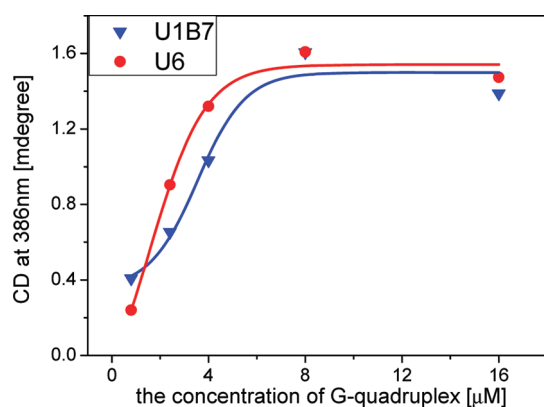


Figure 9. The fitting plot of CD signal at 386 nm against the concentration of G-quadruplexes of U1B7 (▼) and U6 (●) in 90 mM pbs-K⁺ solution at 25 °C.

binding to G-quadruplex based on specific loop interactions was identified. The new G-quadruplex ligand, MACP6, represents a versatile and promising scaffold. For other well-known macrocycle G-quadruplex ligands, such as telomestatin^{16,17} and HXDV,¹⁹ their high G-quadruplex-selectivity relies mainly on the shape matching between the macrocycles and the G-quartet. As for MACP6, its preferred binding to G-quadruplex against duplex DNA is resulted mostly from the loop binding mode, and molecular size of MACP6 also contributes to their binding. Additionally, loops in the G-quadruplexes and the nucleotides nature in the loop also play important roles in the selective binding of

MACP6 to various G-quadruplexes. Similar conclusion have been drawn in the case of TMPyP4,^{51,52} where the loop orientation and loop length of the G-quadruplex have been verified to strongly affect the binding affinity and selectivity, and disubstituted acridine⁵³ where the nature of the loop significantly influences the binding selectivity to particular G-quadruplex motifs. Furthermore, discrimination of hybrid/antiparallel conformations of H22 is achieved by MACP6. Clearly, shape matching between the molecular frame of the ligands and the G-quartet, and the preferred loop binding between the ligands and G-quadruplexes should be two possible ways to improve the G-quadruplex-selectivity of the new G-quadruplex ligands. This would be a guideline to design novel G-quadruplex ligands with higher selectivity.

■ ASSOCIATED CONTENT

S Supporting Information. The CD spectra of MACP6 with other G-quadruplexes. NMR and ESI-MS spectra of MACP6. ¹H-NMR spectra and modeling results of MACP6 with G-quadruplexes. This material is available free of charge via the Internet at <http://pubs.acs.org>.

■ AUTHOR INFORMATION

Corresponding Author

*(Y.-L.T.) E-mail: tangyl@iccas.ac.cn; phone: +86/10/62522090; fax: +86/10/62522090. (M.-X.W.) E-mail: wangmx@mail.tsinghua.edu.cn.

■ ACKNOWLEDGMENT

This work is supported by the Major Research Program of the National Natural Science Foundation of China (Grant No. 91027033) and the General Program of the National Natural Science Foundation of China (Grant No. 81072576).

■ REFERENCES

- (1) Brunori, M.; Luciano, P.; Gilson, E.; Geli, V. *J. Mol. Med.* **2005**, *83*, 244–257.
- (2) Blackburn, E. H. *Nature* **1991**, *350*, 569–573.
- (3) Zahler, A. M.; Williamson, J. R.; Cech, T. R.; Prescott, D. M. *Nature (London)* **1991**, *350*, 718–720.
- (4) Schultze, P.; Macaya, R. F.; Feigon, J. *J. Mol. Biol.* **1994**, *235*, 1532–1547.
- (5) Siddiqui-Jain, A.; Grand, C. L.; Bearss, D. J.; Hurley, L. H. *Proc. Natl. Acad. Sci. U.S.A.* **2002**, *99*, 11593–11598.
- (6) Dai, J. X.; Dexheimer, T. S.; Chen, D.; Carver, M.; Ambrus, A.; Jones, R. A.; Yang, D. Z. *J. Am. Chem. Soc.* **2006**, *128*, 1096–1098.

- (7) Patel, D. J.; Phan, A. T.; Kuryavyi, V. *Nucleic Acids Res.* **2007**, *35*, 7429–7455.
- (8) Monchaud, D.; Teulade-Fichou, M. P. *Org. Biomol. Chem.* **2008**, *6*, 627–636.
- (9) Zhang, X. F.; Xiang, J. F.; Tian, M. Y.; Tang, Y. L. *Chin. Sci. Bull. (Chin. Ed.)* **2009**, *54*, 1374–1386.
- (10) Fedoroff, O. Y.; Salazar, M.; Han, H. Y.; Chemeris, V. V.; Kerwin, S. M.; Hurley, L. H. *Biochemistry* **1998**, *37*, 12367–12374.
- (11) Gavathiotis, E.; Heald, R. A.; Stevens, M. F. G.; Searle, M. S. *J. Mol. Biol.* **2003**, *334*, 25–36.
- (12) Dixon, I. M.; Lopez, F.; Tejera, A. M.; Esteve, J. P.; Blasco, M. A.; Pratviel, G.; Meunier, B. *J. Am. Chem. Soc.* **2007**, *129*, 1502–1503.
- (13) Li, Q.; Xiang, J.; Li, X.; Chen, L.; Xu, X.; Tang, Y.; Zhou, Q.; Li, L.; Zhang, H.; Sun, H.; Guan, A.; Yang, Q.; Yang, S.; et al. *Biochimie* **2009**, *91*, 811–819.
- (14) Brassart, B.; Gomez, D.; De Cian, A.; Paterski, R.; Montagnac, A.; Qui, K. H.; Temime-Smaali, N.; Trentesaux, C.; Mergny, J. L.; Gueritte, F. O.; et al. *F. Mol. Pharmacol.* **2007**, *72*, 631–640.
- (15) Zhang, H.; Xiang, J. F.; Hu, H. Y.; Li, L.; Jin, X.; Liu, Y.; Li, P. F.; Tang, Y. L.; Chen, C. F. *Biochemistry* **2010**, *49*, 10351–10353.
- (16) Kim, M. Y.; Vankayalapati, H.; Kazuo, S.; Wierzb, K.; Hurley, L. H. *J. Am. Chem. Soc.* **2002**, *124*, 2098–2099.
- (17) Gomez, D.; O'Donohue, M. F.; Wenner, T.; Douarre, C.; Macadre, J.; Koebel, P.; Giraud-Panis, M. J.; Kaplan, H.; Kolkes, A.; Shin-Ya, K.; et al. *Cancer Res.* **2006**, *66*, 6908–6912.
- (18) Jantos, K.; Rodriguez, R.; Ladame, S.; Shirude, P. S.; Balasubramanian, S. *J. Am. Chem. Soc.* **2006**, *128*, 13662–13663.
- (19) Barbieri, C. M.; Srinivasan, A. R.; Rzuczek, S. G.; Rice, J. E.; LaVoie, E. J.; Pilch, D. S. *Nucleic Acids Res.* **2007**, *35*, 3272–3286.
- (20) Harrowfield, J.; Vicens, J. *Tetrahedron* **2007**, *63*, 10719–10719.
- (21) de Fátima, A.; Fernandes, S. A.; Sabino, A. A. *Curr. Drug Discovery Technol.* **2009**, *6*, 151–170.
- (22) Böhmer, V. *Angew. Chem., Int. Ed.* **1995**, *34*, 713–745.
- (23) Shinkai, S.; Ikeda, A. *Chem. Rev.* **1997**, *97*, 1713–1734.
- (24) Miyazaki, Y.; Kanbara, T.; Yamamoto, T. *Tetrahedron Lett.* **2002**, *43*, 7945–7948.
- (25) Zhang, E. X.; Wang, D. X.; Zheng, Q. Y.; Wang, M. X. *Org. Lett.* **2008**, *10*, 2565–2568.
- (26) Phan, A. T.; Kuryavyi, V.; Burge, S.; Neidle, S.; Patel, D. J. *J. Am. Chem. Soc.* **2007**, *129*, 4386–4392.
- (27) Phan, A. T.; Modi, Y. S.; Patel, D. J. *J. Am. Chem. Soc.* **2004**, *126*, 8710–8716.
- (28) Beger, R. D.; Marathias, V. M.; Volkman, B. F.; Bolton, P. H. *J. Magn. Reson.* **1998**, *135*, 256–259.
- (29) Xu, Y.; Noguchi, Y.; Sugiyama, H. *Bioorg. Med. Chem.* **2006**, *14*, 5584–5591.
- (30) Rujan, I. N.; Meleney, J. C.; Bolton, P. H. *Nucleic Acids Res.* **2005**, *33*, 2022–2031.
- (31) Luu, K. N.; Phan, A. T.; Kuryavyi, V.; Lacroix, L.; Patel, D. J. *J. Am. Chem. Soc.* **2006**, *128*, 9963–9970.
- (32) Phan, A. T.; Kuryavyi, V.; Luu, K. N.; Patel, D. J. *Nucleic Acids Res.* **2007**, *35* (50), 6517–6525.
- (33) Phan, A. T.; Luu, K. N.; Patel, D. J. *Nucleic Acids Res.* **2006**, *34*, 5715–5719.
- (34) Phan, A. T.; Patel, D. J. *J. Am. Chem. Soc.* **2003**, *125*, 15021–15027.
- (35) Parkinson, G. N.; Cuenca, F.; Neidle, S. *J. Mol. Biol.* **2008**, *381*, 1145–1156.
- (36) Gavathiotis, E.; Searle, M. S. *Org. Biomol. Chem.* **2003**, *1*, 1650–1656.
- (37) Ambrus, A.; Chen, D.; Dai, J. X.; Jones, R. A.; Yang, D. Z. *Biochemistry* **2005**, *44*, 2048–2058.
- (38) Parkinson, G. N.; Lee, M. P.; Neidle, S. *Nature* **2002**, *417*, 876–880.
- (39) Otsuka, H.; Shinkai, S. *J. Am. Chem. Soc.* **1996**, *118*, 4271–4275.
- (40) Berova, N.; Nakanishi, K.; Woody, R. W. Eds. *Circular Dichroism: Principles and Applications*, 2nd ed.; Wiley-VCH: New York, 2000.
- (41) Davis, J. T. *Angew. Chem., Int. Ed.* **2004**, *43*, 668–698.
- (42) Tanious, F. A.; Ding, D. Y.; Patrick, D. A.; Tidwell, R. R.; Wilson, W. D. *Biochemistry* **1997**, *36*, 15315–15325.
- (43) Gellert, M.; Lipsett, M. N.; Davies, D. R. *Proc. Natl. Acad. Sci. U.S.A.* **1962**, *48*, 2013–2018.
- (44) Meier, J.; Higuchi, T. *J. Pharm. Sci.* **1965**, *54*, 1183–1186.
- (45) Burge, S.; Parkinson, G. N.; Hazel, P.; Todd, A. K.; Neidle, S. *Nucleic Acids Res.* **2006**, *34*, 5402–5415.
- (46) Keniry, M. A. *Biopolymers* **2000**, *56*, 123–146.
- (47) Gabelica, V.; Baker, E. S.; Teulade-Fichou, M. P.; De Pauw, E.; Bowers, M. T. *J. Am. Chem. Soc.* **2007**, *129*, 895–904.
- (48) Rankin, S.; Reszka, A. P.; Huppert, J.; Zloh, M.; Parkinson, G. N.; Todd, A. K.; Ladame, S.; Balasubramanian, S.; Neidle, S. *J. Am. Chem. Soc.* **2005**, *127*, 10584–10589.
- (49) Seenisamy, J.; Rezler, E. M.; Powell, T. J.; Tye, D.; Gokhale, V.; Joshi, C. S.; Siddiqui-Jain, A.; Hurley, L. H. *J. Am. Chem. Soc.* **2004**, *126*, 8702–8709.
- (50) Wang, Y.; Patel, D. J. *Structure* **1993**, *1*, 263–282.
- (51) Arora, A.; Maiti, S. *J. Phys. Chem. B* **2008**, *112*, 8151–8159.
- (52) Arora, A.; Maiti, S. *J. Phys. Chem. B* **2009**, *113*, 8784–8792.
- (53) Campbell, N. H.; Patel, M.; Tofa, A. B.; Ghosh, R.; Parkinson, G. N.; Neidle, S. *Biochemistry* **2009**, *48*, 1675–1680.